Suppression of moiré patterns in scanned halftone images by double scans with grid movements ☆

James Ching-Yu Yang [1], Wen-Hsiang Tsai

Department of Computer and Information Science, National Chiao Tung University, Hsinchu, Taiwan 300, People's Republic of China

Abstract

Moiré patterns often appear in images obtained from scanning printings on magazines or newspapers. The patterns do not exist in the original printings but come from alias sampling of the screened halftone pictures. A new method of scanning is proposed to suppress the moiré patterns. First, the Fourier analyses of both screening and scanning are presented, from which the new moiré suppression scanning method is derived. The method employs a double-scan process. In the second scan, the scan position is shifted by half of the sampling grid distance of the first scan in either or both of the horizontal and vertical directions. Then by averaging the images of the two scans, most of the moiré fringes can be removed. Some experimental results are shown to demonstrate the feasibility of the proposed approach. © 1997 Published by Elsevier Science B.V.

Keywords: Moiré pattern; Suppression; Scanning; Printing; Screened pictures; Fourier analysis

1. Introduction

Most printed articles are produced by the planographic printing technique, in which only a few color inks are used. By this technique, we can hardly print images using as many colors as in the source images. For example, a common gray-scale image contains 256 gray levels. It is necessary to perform a screening process to translate a gray-scale image into a halftone image. A halftone image is a high-frequency black and white image, in which gray intensities are represented as black dots of different sizes. The black dots in a halftone image are spread periodically, orthogonally, and mostly with the angle of 45° in order to comfort the human eyes. The halftoning technology has been reviewed by Jones (1994). Practically, a software or a machine, called raster image processor (RIP), is required to generate halftone images. The generated halftone image can then be printed by the planographic technique. Fink (1992) has described the screening process of the RIP. An example of the halftone image is given in Fig. 1.
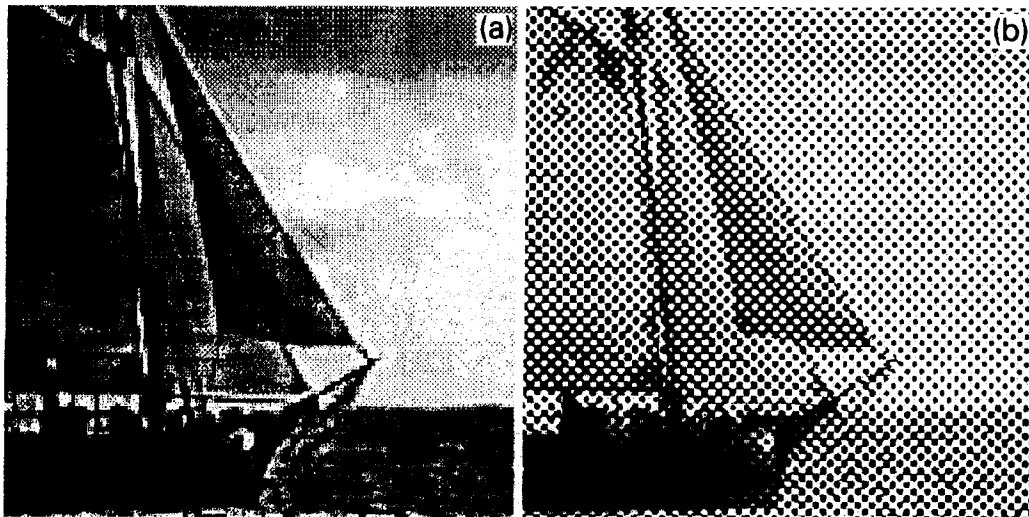
Fig. 1. An example of a gray-scale image and its corresponding halftone image. (a) Original gray-scale image. (b) Corresponding halftone image.

When we scan an image with periodic structures, aliasing is unavoidable and additional moiré patterns will usually appear in the scanning result. This problem has been a subject in the literature (e.g., Rosenfeld, 1982). Because screen dots repeat periodically in a halftone image, scanning a halftone image will generate additional moiré patterns. Fourier analysis can be employed to describe this phenomenon. In this paper, the Fourier analyses of both the screening and the scanning processes will be presented.

According to the structure of scanner hardware, the image scanning process can be divided into three major stages. The first stage is pre-filtering which is an optical process related to the characteristics of the scanner lens. For a large drum scanner, a user can adjust the focus and the aperture of the lens to make the scanning result sharper or smoother. The next stage is the sampling process which is realized by motor moving or CCD arrangement. A user can adjust the scanning resolution to change sampling grids. The brightness values of the scanned picture are quantized into digital values. The final stage is post-filtering which is a software process employed to correct digital image values by gamma correction, look up tables, or other filters. The moiré phenomenon mainly comes from the thresholding step in screening and the sampling step in scanning. Some works proposed to suppress moiré patterns are reviewed in the following.

(1) Smoothing is a natural way to remove high-frequency noise. A scanner operator usually adjusts the focus or the aperture in the pre-filtering stage to smooth the scanning result in order to suppress the moiré phenomenon. As is well known, smoothing is a low-pass filter in the frequency domain. It reduces the high-frequency halftone screen signals, removes most periodic structures of the image, and makes the sampling yield less alias. On the other hand, there are some problems which are related to smoothing. First, the image will be blurred. Next, it is difficult to perform good aperture or focus adjustment. Besides, only high-end drum scanners support these kinds of adjustments in the pre-filtering stage.

(2) Using inverse halftoning as a post-filter is possible. First, all the detail of the halftone image is scanned with higher resolution. By analysis of each screen dot, it is possible to derive a corresponding gray-scale image. Miceli and Parker (1992) and Fan (1992) proposed algorithms to do this. Some drawbacks of these methods are that additional long processing time may be required and that high-resolution scanning takes longer time and larger memory space.

(3) Shu and Yeh (1989) analyzed possible factors that cause moiré patterns. They figured out a rule to formulate the relationship between scanning resolution, screening resolution, their angles, and moiré visibility.

A suggestion to select a scanning resolution was proposed to make scanning yield minimum visibility of moiré patterns.

(4) Russ (1993) proposed filtering of images in the frequency domain. Periodic information in the frequency domain is removed by manual masking operations. However, it is difficult to determine in the frequency domain where is the information that causes moiré patterns in the original image.

Most of the above methods are based on single scanning results. In fact, additional scans of different configurations are also helpful to provide information for moiré suppression. A new method is proposed in this paper that employs a double-scan process and yields good suppression of moiré patterns. An additional scan process is introduced, in which the scan position is shifted by half of the distance between two neighboring scan grids in either or both of the horizontal and vertical directions. The second scanned image contains moiré patterns which complement those of the first scanned image. By averaging these two images, most prominent moiré patterns can be removed. Detailed theoretic analyses based on the Fourier transforms of the image data are also provided to explain the function of the proposed moiré pattern suppression method.

The remainder of this paper is organized as follows. In Section 2, we formulate the screening and the scanning processes. By Fourier analysis, we show how moiré patterns are generated during halftone image scanning. In Section 3, we describe the proposed moiré suppression method using scan grid movements. In Section 4, some experimental results are shown, followed by conclusions in Section 5.

2. Fourier analysis of moiré phenomenon

2.1. Fourier analysis of screening

Halftoning is a thresholding process that converts a gray-scale image $g(r)$ into a binary image $h(r)$ consisting of screen dots. Thresholding is performed using a thresholding function $s(r)$. The corresponding binary image value is set to 0 (black) if the intensity value of a pixel in the original gray-scale image is smaller than or equal to that of the thresholding function value; and is set to 1 (white) if the intensity value is larger than that of the thresholding function value, as described in the following:

$$h(r) = \begin{cases} 0, & \text{if } g(r) \leqslant s(r), \\ 1, & \text{otherwise.} \end{cases} \tag{1}$$

Since the screen dots are spread uniformly and orthogonally, they can be imagined to be arranged on a screen lattice. And the thresholding function $s(r)$ can be defined as a convolution of a screen dot function and the screen lattice:

$$s(r) = s_d(r) * \sum_{m=-\infty}^{\infty} \sum_{n=-\infty}^{\infty} \delta(r - mr_1 - nr_2), \tag{2}$$

where $s_d(r)$ is the screen dot function which defines how the screen dots extend; and r_1 and r_2 are two orthogonal basis vectors of the screen lattice which is defined as a combination of mr_1 and nr_2, where m and n are integer numbers. Fig. 2 shows the thresholding function, defined in Eq. (2), in the spatial domain along the direction of r_1. Notice that the screen dot function $s_d(r)$ is repeated on the screen lattice.
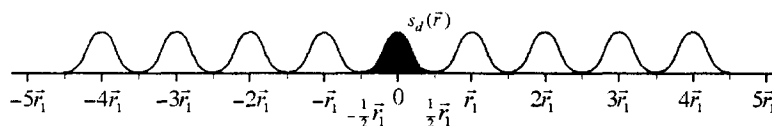

Fig. 2. Thresholding function in the direction of r_1 in spatial domain.

To make the analysis easier, Eq. (1) can also be written in the following form:

$$h(r) = \begin{cases} 0, & \text{if } g_n(r)s(r) \geqslant 1, \\ 1, & \text{otherwise}, \end{cases} \tag{3}$$

where $g_n(r)$ is the reciprocal function of the original gray-scale image, assuming $g(r) > 0$, defined by

$$g_n(r) = \frac{1}{g(r)}.$$

The Fourier transform of the term $g_n(r)s(r)$ in Eq. (3) is as follows:

$$\mathscr{F}\{g_n(r)s(r)\} = G_n(w) * \left[S_d(w) \times C_1 \sum_{k=-\infty}^{\infty} \sum_{l=-\infty}^{\infty} \delta(w - kw_1 - lw_2) \right], \tag{4}$$

where $G_n(w)$ is the Fourier transform of the reciprocal gray-scale image $g_n(r)$; $S_d(w)$ is the Fourier transform of the screen dot function $s_d(r)$; w_1 and w_2 are the reciprocal basis vectors derived from the basis vectors r_1 and r_2; and C_1 is a constant.

Fig. 3(a) shows the relation among the Fourier transforms of the screen dot function, the screen lattice, and the thresholding function in the 1D case. The convolution of $G_n(w)$ with the impulses of the thresholding function $s(r)$ results in a function described by Eq. (4) and shown in Fig. 3(b). Again, the Fourier transform $G_n(w)$ of the reciprocal gray-scale image $g_n(r)$ normally has less power in the high-frequency range than in the low-frequency range. A convolution of it with an impulse signal of $s(r)$ at $kw_1 + lw_2$ produces a signal component at frequency $kw_1 + lw_2$, whose magnitude decreases as k and l increase.

Now, check Eq. (3) again. When thresholding is applied to $g_n(r)s(r)$, signal hills are transformed into black screen dots. The thresholding operation does not break the periodical structure. The thresholding result has
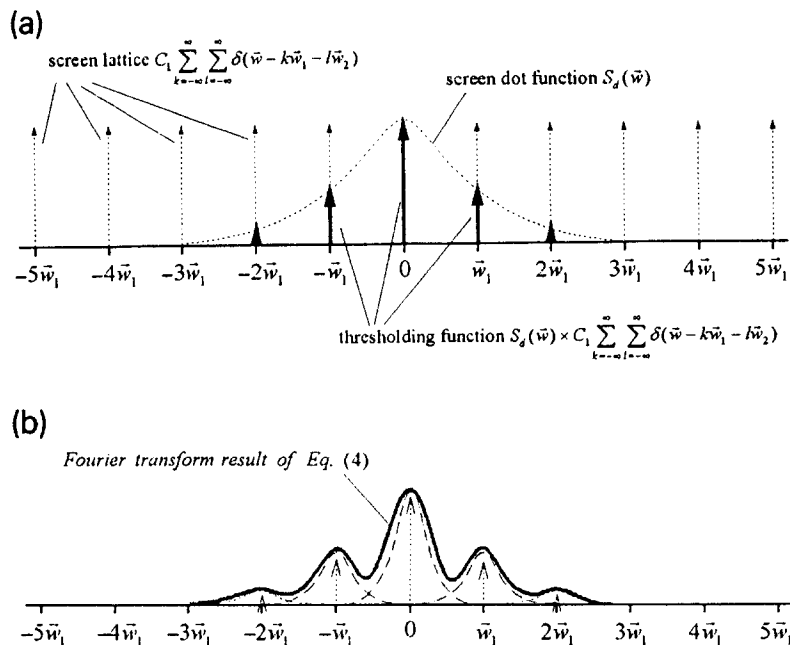

Fig. 3. Fourier transforms of thresholding function and result of Eq. (4). (a) Relation among Fourier transforms of screen dot function (dashed hill function), screen lattice (dashed impulses), and thresholding function in frequency domain (solid impulses) in the 1D case. (b) Fourier transform described by Eq. (4), a convolution of the shape shown in (a) and $G_n(w)$.
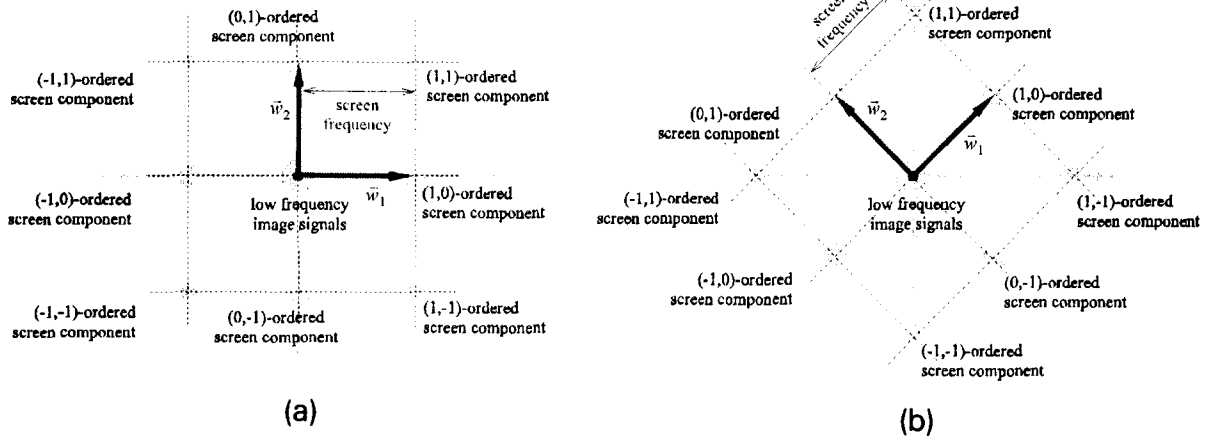
Fig. 4. The screen components of screened images in frequency domain (larger dots indicate stronger signals). (a) The screen components of a 0° screened image. (b) The screen components of a 45° screened image.

corresponding signal components at $kw_1 + lw_2$ in the frequency domain. We call such signal components as (k,l)-ordered screen components in the frequency domain. Fig. 4 shows a 2D illustration of the most significant screen components of a 0° and a 45° screened halftone image in the frequency domain. Larger dots indicate stronger signals.

2.2. Fourier analysis of scanning

As described before, there are three stages in the scanning process. Post-filtering does not affect the moiré pattern. The following equation models the first two stages of scanning, namely, pre-filtering and sampling:

$$g'(r) = [h(r) * a(r)] \times \sum_{m=-\infty}^{\infty} \sum_{n=-\infty}^{\infty} \delta(r - m\alpha_1 - n\alpha_2),$$ (5)

where α_1 and α_2 are the basis vectors of the scan grids; $a(r)$ is the aperture function which defines the aperture transmittance of the scanner lens; $h(r)$ is the source halftone image produced by the raster image processor and printed on paper, which is described by Eq. (3); and $g'(r)$ is the gray-scale image resulting from scanning. The first part $h(r) * a(r)$ in Eq. (5), the convolution, models the pre-filtering in the scanning process. Light reflected from the printed halftone image is collected by the optical structure of the scanner. After that, light is sampled at each position of $m\alpha_1 + n\alpha_2$, where m and n are integers. Its magnitude reflects the focus and the aperture characteristics of the scanner lens and is a distance function. The larger the distance from the center of the sampling point, the less light can be transmitted.

The Fourier transform of Eq. (5) is

$$G'(w) = [H(w) \times A(w)] * C_2 \sum_{k=-\infty}^{\infty} \sum_{l=-\infty}^{\infty} \delta(w - ku_1 - lu_2),$$ (6)

where $H(w)$ is the Fourier transform of $h(r)$; $A(w)$ is the Fourier transform of $a(r)$; u_1 and u_2 are the reciprocal basis vectors derived from α_1 and α_2; and C_2 is a constant.

The first part $H(w) \times A(w)$ of Eq. (6), the product of the aperture function and the original halftone image in the frequency domain, is shown in Fig. 5 for the 1D case. According to the previous discussion, the halftone image $H(w)$ has signal components at frequencies $mw_1 + nw_2$, i.e., the (m, n)-ordered screen components. The
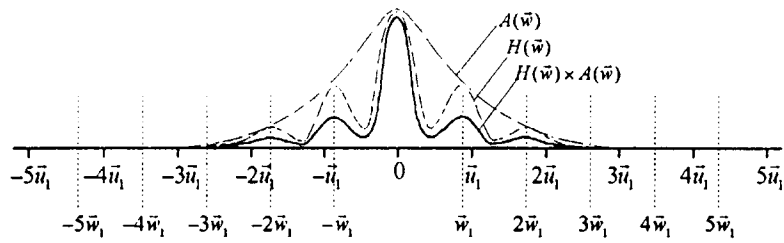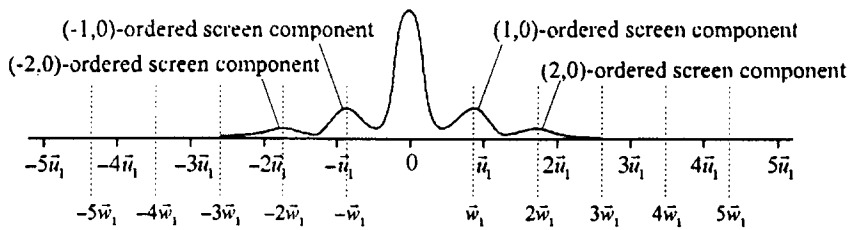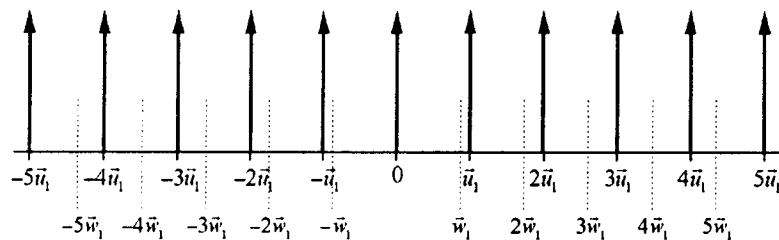
Fig. 5. $H(w) \times A(w)$ in frequency domain.

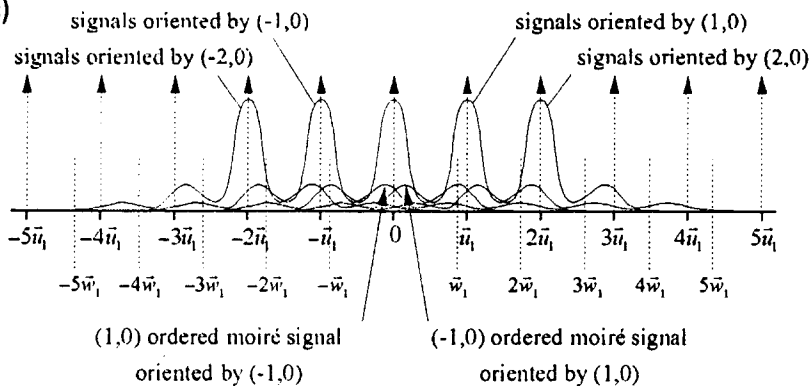Fig. 6. 1D illustration of moiré signal generation for a scan of a $0°$ screened halftone image. (a) The result of $H(w) \times A(w)$ in frequency domain. (b) The scanning lattice. (c) The convolution of (a) and (b).
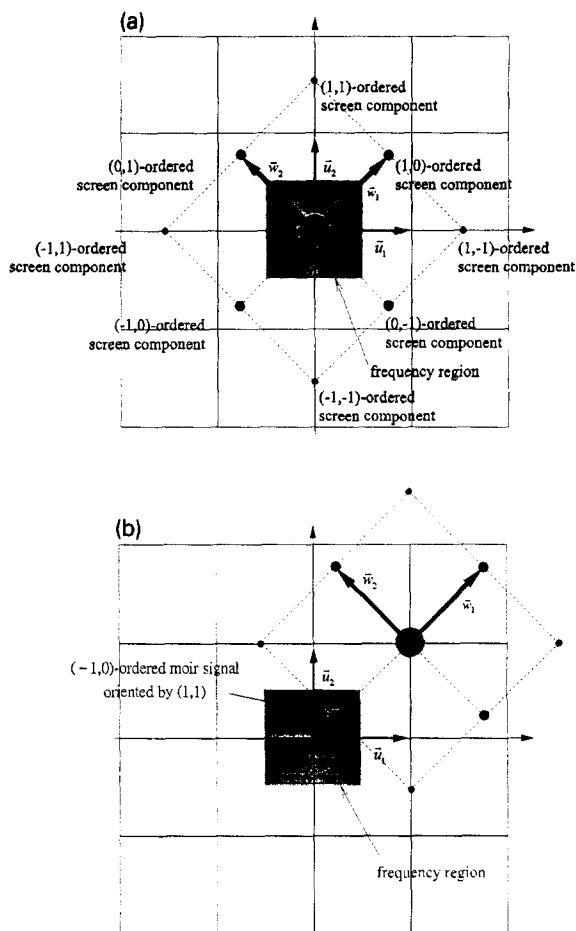
Fig. 7. Illustration of moiré pattern generation in the 2D case for a scan of a 45° screened halftone image. (a) Halftone signals in frequency domain. (b) Result of convolution of (a) with impulse $\delta(u_1 + u_2)$ (note that the $(-1, 0)$-ordered screen component is shifted into the low-frequency region that effects as a moiré signal).

product $H(w) \times A(w)$ should also have the corresponding signal components at $mw_1 + nw_2$. When the product is convolved with the lattices spread by basis vectors u_1 and u_2 as described in Eq. (6), the signal components of $H(w) \times A(w)$ centered at $mw_1 + nw_2$ are duplicated at each point of the scan grids. When w_1 and w_2 do not match u_1 and u_2, respectively, signal components overlap and aliasing occurs. That is, some additional signals are shifted into the low-frequency area as a result of the convolution of $H(w) \times A(w)$ with $\delta(w - ku_1 - lu_2)$ and yield moiré patterns. We call such signals (m, n)-ordered moiré signals oriented by (k, l). Fig. 6 illustrates the phenomenon in the 1D case along the u_1 direction for a scan of a 0° screened halftone image. It is pointed out here that it is the $(\pm 1, 0)$-ordered moiré signals oriented by $(\pm 1, 0)$ placed in the low-frequency area that introduce the most prominent moiré patterns. Fig. 7 illustrates the phenomenon in the 2D case, where the convolution of the halftone image signal components with impulse $\delta(u_1 + u_2)$ causes the shift of the original $(-1, 0)$-ordered signal component into the low-frequency area which becomes the $(-1, 0)$-ordered moiré signal oriented by $(1, 1)$.

3. Proposed double-scan method with grid movements

The resulting moiré pattern will become different if we move the sampling grids. In the following analysis, it will be proved that if we move the sampling grids half of the grid distance and rescan the image, the resulting moiré pattern will mostly be negative with respect to that of the first scan. Darker moiré patterns will become lighter, and lighter moiré patterns become darker. By averaging the original image and the rescanned one, a better image with less moiré phenomenon can be obtained. This is the basic idea of the proposed approach. More general cases of grid movements will also be analyzed in this section.

3.1. Scan grid movements

When the scan grids are moved by an arbitrary *displacement vector* d, the grids in Eq. (5) should be modified into the following form:

$$\sum_{m=-\infty}^{\infty} \sum_{n=-\infty}^{\infty} \delta(r - m\alpha_1 - n\alpha_2 - d). \tag{7}$$

And its Fourier transform becomes

$$\left[C_2 \sum_{k=-\infty}^{\infty} \sum_{l=-\infty}^{\infty} \delta(w - ku_1 - lu_2) \right] e^{-j2\pi d \cdot w}, \tag{8}$$

whose nonzero values occur at frequency positions $ku_1 + lu_2$ where k and l are integers. The term $d \cdot w$ can be written as

$$d \cdot w = d \cdot ku_1 + d \cdot lu_2. \tag{9}$$

The scan grids can be moved along the directions of u_1, u_2, or $u_1 + u_2$. The effects of these three types of grid movements are discussed in the following.

3.1.1. Horizontal grid movement

The first type is horizontal grid movement, in which the scan grids are moved horizontally by half of the grid distance, i.e., the displacement vector d equals $\frac{1}{2}\alpha_1$. Here, d is orthogonal to u_2, so the term $d \cdot ku_2$ becomes 0. And Eq. (9) becomes $\frac{1}{2}k$. Also, the last term $e^{-j2\pi d \cdot w}$ of Eq. (8) becomes

$$e^{-j2\pi d \cdot w} = e^{-j\pi k} = \begin{cases} 1, & \text{when } k \text{ is an even number;} \\ -1, & \text{when } k \text{ is an odd number.} \end{cases} \tag{10}$$

3.1.2. Vertical grid movement

The second type is vertical grid movement, in which the scan grids are moved vertically by half of the grid distance, i.e., the displacement vector d equals $\frac{1}{2}\alpha_2$. An analysis similar to that for the horizontal grid movement leads to the following result:

$$e^{-j2\pi d \cdot w} = e^{-j\pi l} = \begin{cases} 1, & \text{when } l \text{ is an even number;} \\ -1, & \text{when } l \text{ is an odd number.} \end{cases} \tag{11}$$

3.1.3. Diagonal grid movement

The third type is diagonal grid movement, in which the scan grids are moved by half of the grid distance in both of the directions of u_1 and u_2, i.e., the displacement vector d equals $\frac{1}{2}(\alpha_1 + \alpha_2)$. Similarly, it is easy to get the following result:

$$e^{-j2\pi d \cdot w} = e^{-j\pi(k+l)} = \begin{cases} 1, & \text{when } k+l \text{ is an even number;} \\ -1, & \text{when } k+l \text{ is an odd number.} \end{cases} \tag{12}$$

3.2. Averaging of two scanning results for 0° screen image

Now, suppose a 0° screen image is rescanned with diagonally moved scan grids. After $H(w) \times A(w)$ is convolved with the term of Eq. (8), as described in Eq. (6), the result of the 1D case along the u_1 direction is shown in Fig. 8. The scan grids along u_1 after being moved are shown in Fig. 8(a). The convolution of $H(w) \times A(w)$ with the moved grids are shown in Fig. 8(b). Comparing the result with Fig. 6(c), we found that the two peaks of $H(w) \times A(w)$ at positions $\pm u_1$, signals oriented by $(\pm 1, 0)$, are complementary to the corresponding ones of $H(w) \times A(w)$ in Fig. 6(c) (i.e., identical in amplitude but different in sign). We can also notice that in the low-frequency area, the $(\pm 1, 0)$-ordered moiré signals oriented by $(\pm 1, 0)$ are also negative with respect to the corresponding ones in Fig. 6(c).

Now, after averaging the results of the original and the second scans, the 1D result is shown in Fig. 9. The screen components oriented by $(2k \pm 1, l)$ are removed by the averaging. Prominent moiré signals that are oriented by $(\pm 1, 0)$ and $(0, \pm 1)$ are also removed.

Fig. 10 shows the example in the 2D case. Fig. 10(a) shows the signals of the original scan. Moiré signals appear in the low-frequency region. As described in Section 3.1.3, the impulses at position (k, l) are negative while $k + l$ are odd numbers. The result of the convolved halftone signals at those position are complementary

Fig. 8. Result of a scan with half grid distance move. (a) The scan grids after being moved by half of the grid distance horizontally. (b) The result of the second scan, the convolution of $H(w) \times A(w)$ and (a).
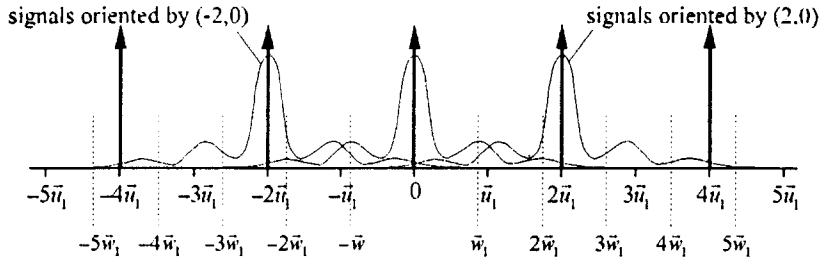
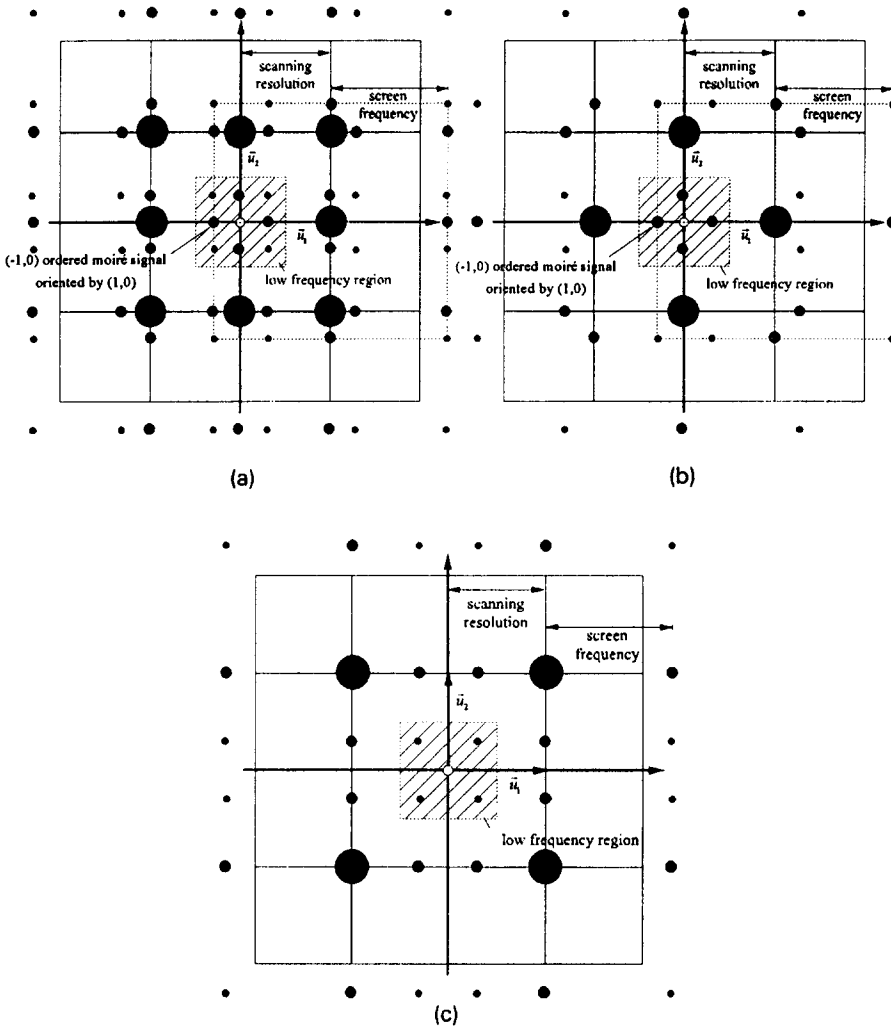Fig. 9. The averaged signals of the two scans.

(a)

(b)

(c)

Fig. 10. 2D illustration of the averaging process proposed to remove moiré signals. (a) Signals of original scan (moiré signals appear in the shaded frequency region). (b) Result of the convolution of the halftone signals with the negative impulses after the scan grids are moved diagonally (all black dots indicate negative values). (c) Result of the averaging process (less moiré signals appear in the low-frequency region).

to the corresponding ones in the original scanning result. Fig. 10(b) shows the result of the convolution of the halftone signals with the negative impulses after the scan grids are moved diagonally. And Fig 10(c) shows the result of the averaging of the two scans. Notice that less moiré signals appear in the low-frequency region.

3.3. Averaging of two scanning results for 45° screen image

Practically, most printed halftone images have 45° screen angles. Also, only a few fixed screen frequencies like 150 or 175 LPI (lines per inch) are used in printing. The locations of the additional moiré signal
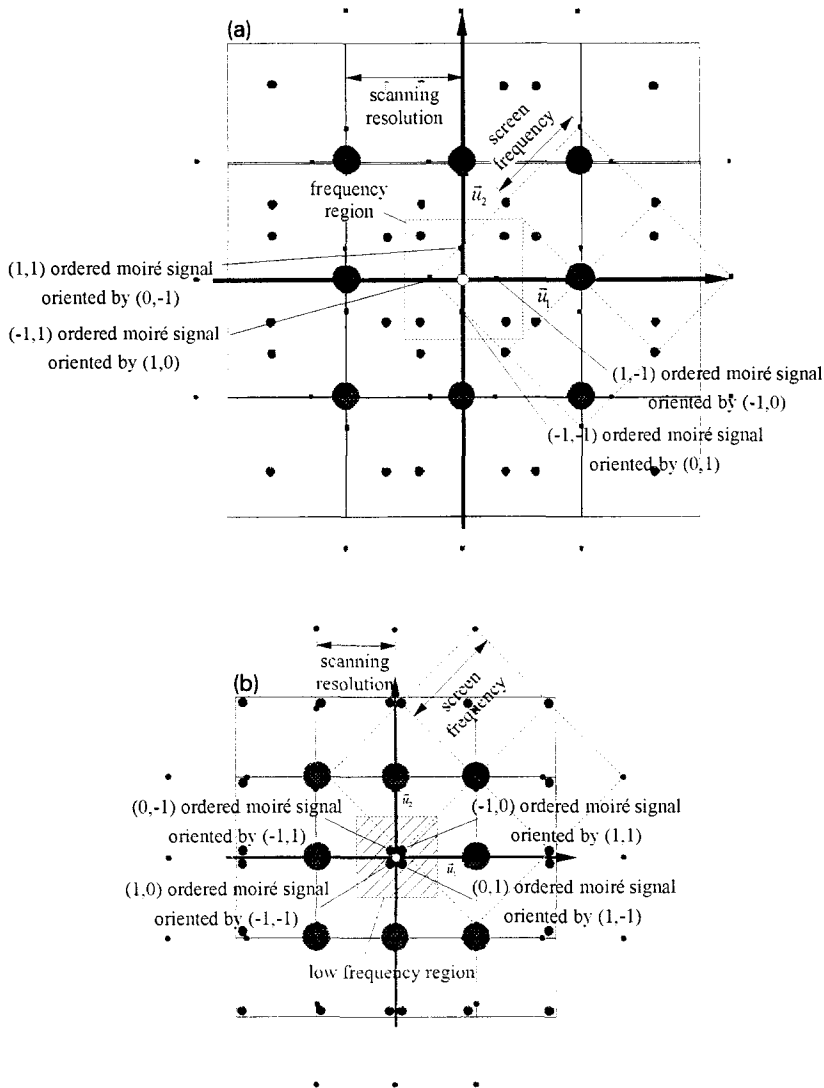

Fig. 11. Two cases of prominent moiré signals resulting from different scanning resolutions. (a) Case I: the moiré signals ordered by $(-1, 1), (-1, -1), (1, -1)$ and $(1, -1)$, and oriented by $(1, 0), (0, 1), (-1, 0)$ and $(0, -1)$, respectively, are the prominent moiré signals. (b) Case II: the moiré signals ordered by $(-1, 0), (0, -1), (0, 1)$ and $(1, 0)$ and oriented by $(1, 1), (-1, 1), (1, -1)$ and $(-1, -1)$, respectively, are the prominent moiré patterns.
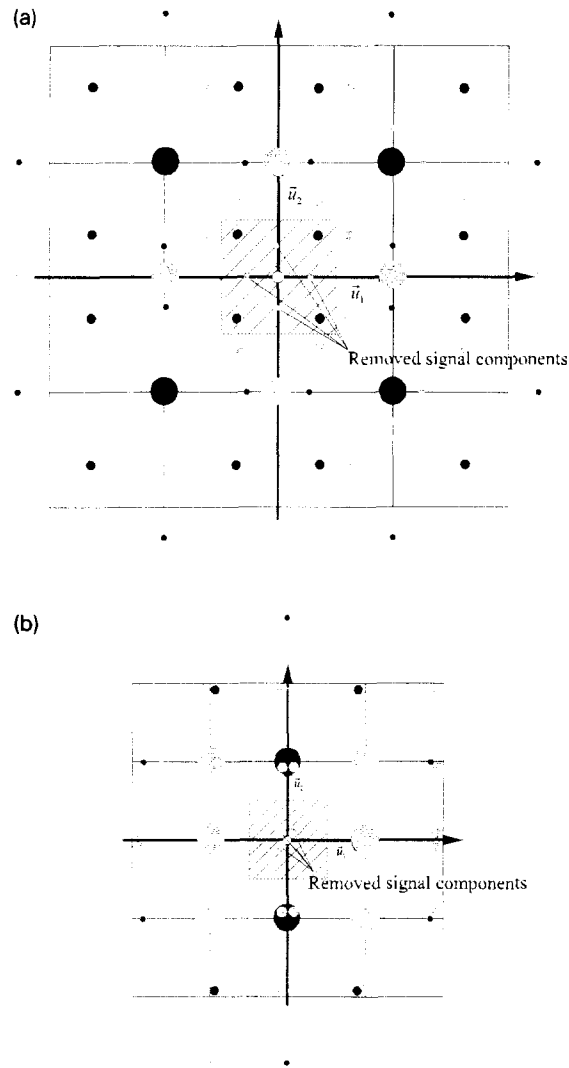
Fig. 12. The result of averaging the original scanning result and the result with scan grid movement. (a) The result of averaging the image in Fig. 15(a) and a scanning result with diagonal grid movement. Signal components in the low frequency area are removed. (b) The result of averaging the image in Fig. 15(b) and a scanning result with horizontal grid movement. Signal components in the low-frequency area are removed.

components vary when the scanning resolution is altered. Two cases of the moiré phenomenon are identified in this study for all possible scanning resolutions.

One case occurs when the scanning resolution is close to $\sqrt{2}$ times of the screen frequency. The moiré signals ordered by $(-1, 1)$, $(-1, -1)$, $(1, -1)$ and $(1, 1)$ and oriented by $(1, 0)$, $(0, 1)$, $(-1, 0)$ and $(0, -1)$, respectively, are placed in the low-frequency area that is sensitive to human eyes. They are the prominent moiré signals. This case is shown in Fig. 11(a).

The other case occurs when the scanning resolution is close to $1/\sqrt{2}$ times of the screen frequency. The moiré signals ordered by $(-1, 0)$, $(0, -1)$, $(0, 1)$ and $(1, 0)$, and oriented by $(1, 1)$, $(-1, 1)$, $(1, -1)$ and $(-1, -1)$, respectively, are placed in the low-frequency area, and become the prominent moiré signals. This case is shown in Fig. 11(b).
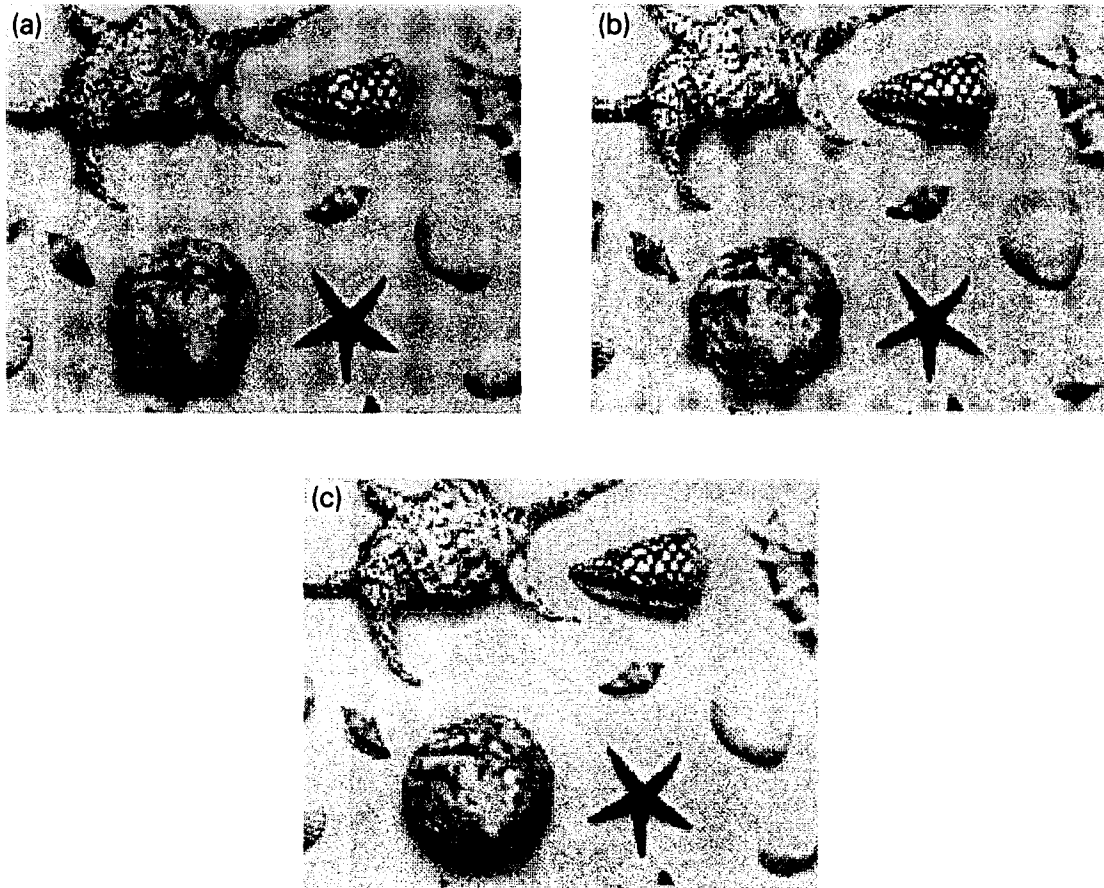
Fig. 13. Test of the proposed approach on a 0° screened halftone image. (a) Original scanning result. (b) Result of second scan with diagonal scan grid movement. (c) Average image of (a) and (b).

To suppress the moiré signals of the first case, we propose to move the scan grids diagonally, perform a new scan, and then average the scanning results together. A better image with less moiré signals will be obtained. Fig. 12(a) shows the average result of the image in Fig. 11(a) and a scanning result with a diagonal grid movement.

For the second case, we propose to move the scan grids horizontally or vertically, perform a new scan, and then average the two scanning results together. Again, a better image with less moiré signals will result. Fig 12(b) shows the average result of the image in Fig. 11(b) and a scanning result with a horizontal grid movement.

To implement the above proposed double-scan process for moiré pattern suppression, the traditional scanning procedure is modified in the following way. First, before the scans, the screen angle and the frequency of the halftone printing are measured by a screen tester that is normally used in a printing shop. Then, a traditional scan is performed to acquire an image of the halftone printing. If moiré patterns are found in the scanning result, a second scan with moved grids is performed to acquire a scanning result that has negative moiré patterns. If the screen angle is 0°, then the grid movement direction should be diagonal. If the screen angle is 45°, an identification of the two cases described before is made by checking the scanning resolution and the screen frequency. Then, either move the scan grids horizontally or diagonally according to the identified case. Finally,
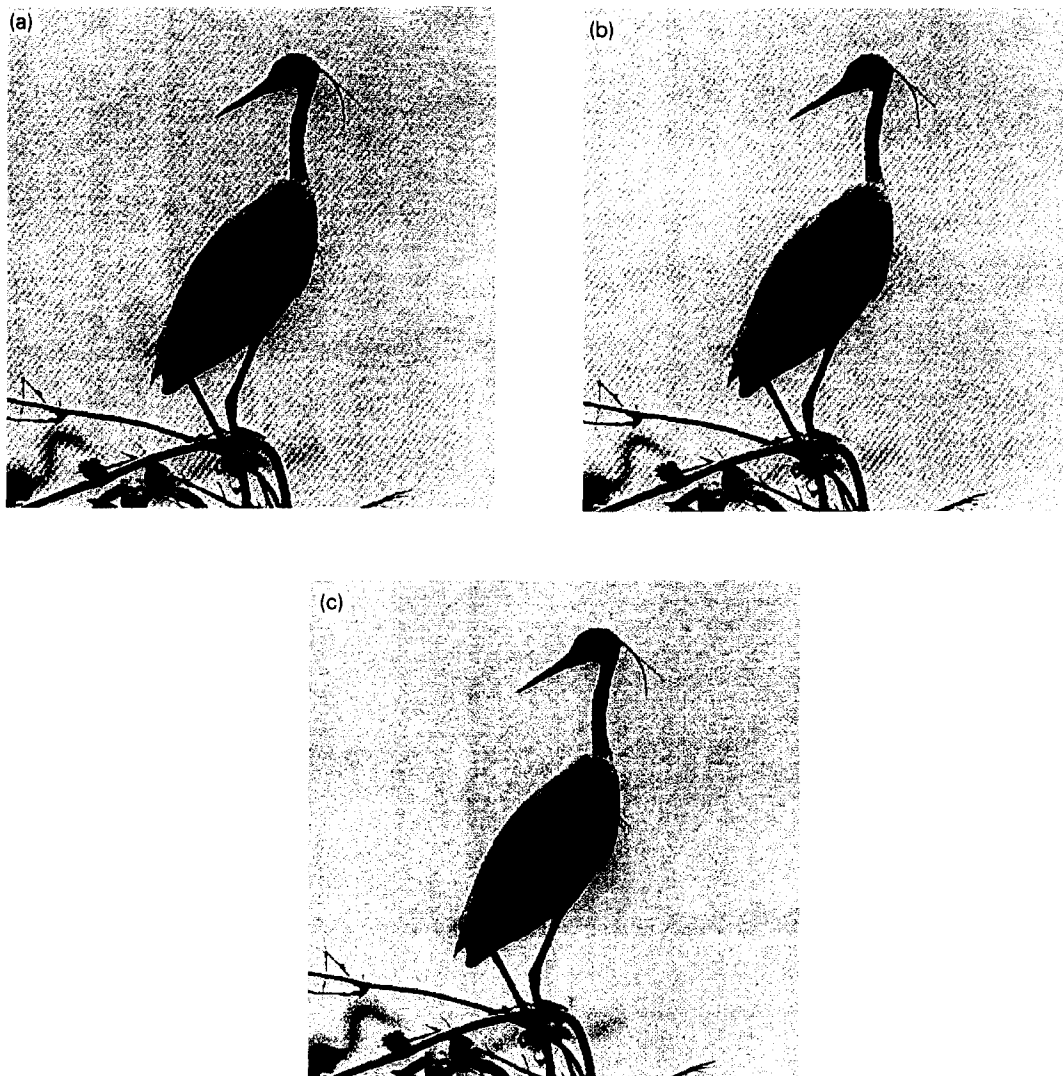
Fig. 14. Test of the proposed approach on a 45° screened halftone image. (a) Original scanning result. (b) Result of second scan with diagonal scan grid movement. (c) Average result of (a) and (b).

average the results of the two scans, and a better result with suppressed most moiré patterns being can be obtained.

4. Experimental results

A series of experiments have been conducted and two results are shown here. Fig. 13 shows the experimental results of applying the proposed method on a printing which is a halftone image with screen frequency 150 LPI and screen angle 0°. Fig. 13(a) shows the original scanning result with scanning resolution 160 DPI, which is full of obvious moiré patterns. Fig. 13(b) shows the result of rescanning the same printing after shifting the scan

grids diagonally by 1/320 inch horizontally and 1/320 inch vertically. Moiré patterns again can be seen obvious. The average image is shown in Fig. 13(c). Comparing it with the result of the first scan shown in Fig. 13(a), we see that the prominent moiré fringes are suppressed.

Fig. 14 shows the results of another experiment on a printing with screen frequency 133 LPI and 45°. Fig. 14(a) shows the original scanning result with resolution 125 DPI which also is full of obvious moiré patterns. Fig. 14(b) shows the result of rescanning the same printing after shifting the grids diagonally by 0.004 inch horizontally and 0.004 inch vertically. This shift can be easily done by moving the scanning window. In our experiments, this was accomplished by adjusting the parameters of the window corner positions during the scanning setup procedure. Moiré patterns again can be seen obvious. The average image is shown in Fig. 14(c) in which no prominent moiré fringes can be seen.

5. Conclusions

When scanning a screened halftone printing, additional moiré patterns will appear in the scanning result. By Fourier analysis, we have shown how these patterns are produced from the alias sampling of the halftone printing by a scanner. A method which employs a double-scan process, followed by an averaging process, has been proposed to suppress the undesired moiré patterns. In the double-scan process, the scan position of the second scan is shifted by half of the sampling grid distance in either or both of the horizontal and vertical directions. In the averaging process, the results of the two scans are averaged and the major moiré patterns can be removed, as proved by the Fourier analysis. Some experimental results showing the feasibility of the approach have also been included.

References

Fan, Z. (1992). Retrieval of gray images from digital halftones. *IEEE Internat. Symp. Circuits and Systems.*
Fink, P. (1992). *Postscript Screening.* Adobe Press, CA.
Jones, P.R. (1994). Evolution of halftoning technology in the United States literature. *Electronic Imaging* 3 (3).
Miceli, C.M. and K.J. Parker (1992). Inverse halftoning. *J. Electronic Imaging* 1 (2).
Rosenfeld, A. and A.C. Kak (1982). *Digital Picture Processing.* Academic Press, New York.
Russ, J.C. (1993). *The Image Processing Handbook.* CRC Press, USA.
Shu, S.P. and C.L. Yeh (1989). Moiré factors and visibility in scanned and printed halftone images. *Optical Engrg.* 28 (7).